Development and Characterization of High Thermal Conductivity Multilayer AlN Substrates

Yasuhiro Kurokawa

Material Development Center, NEC Corporation

1-1, Miyazaki 4-chome, Miyamae-ku, Kawasaki city 213 Japan

ABSTRACT

Recent trend on the development of high thermal conductivity substrates is introduced first. High thermal conductivity AlN substrates, which have thermal conductivity of 160~260 W/mK, have been developed by NEC Corporation. The AlN substrates have several excellent characteristics at room temperature, such as high thermal conductivities over 10 times that of Al_2O_3, a thermal expansion coefficient close to silicon, high electrical insulation resistivity, low dielectric constant and loss, good mechanical properties and non-toxicity.

Multilayer AlN substrates have been developed by co-firing AlN green sheets screen-printed with W thick-film paste. The properties of the substrate, such as electrical resistivity and adhesion of W conductor and the camber of the substrate, were investigated. The chemistry and structure at the AlN-W interface to characterize the high adhesion are discussed.

1. Introduction

The ever increasing demand for electronic circuit miniaturization is continuing for advanced electronic devices. However as a result of increasing circuit density and power on silicon chips, heat dissipation from the chips is becoming critical. In electronic devices, heat dissipation through the substrate is one of the best ways to achieve efficient thermal management in microcircuits. High thermal conductivity substrates will enable heat to be readily dissipated from the chips.

Nowadays, Al_2O_3 ceramics (alumina) with thermal conductivity of 20 W/mK at room temperature has been dominant among substrate materials. In some cases, BeO ceramics (beryllia) has been used, in spite of its toxic nature, because it has high thermal conductivity of 260 W/mK. Recently high thermal conductivity substrates, such as SiC and AlN substrates, have been developed in Japan [1,2,3,4,5,6]. Table 1 summarizes the recent trend on the development of high thermal conductivity substrates. The SiC substrate, which has excellent properties for packaging material, such as high thermal conductivity of 270 W/mK, high electrical insulation resistivity, a thermal expansion coefficient close to that of silicon chip, and high mechanical strength, has been developed. However, it has disadvantages that the dielectric constant and loss are extremely high and the multilayer substrate can not come true through a hot press process. On the other hand, aluminum nitride (AlN) substrates overcame these problems and showed superior properties to Al_2O_3, though the thermal conductivities were not as high as that of BeO at the first stage [2,3,4,5]. Recently the thermal conductivities of AlN increased remarkable in a few years in Japan by improvement of raw AlN powder and sintering process and by utilizing effective sintering additives, such as CaC_2, CaO and Y_2O_3, and finally it became close to that of BeO [6,7,8,9,10]. Further, various applications and evaluations, such as heat sinks, cerdip package, flat package, multilayer multichip package, PGA package and multilayer PGA package, were investigated [5,6,7,8,9,10]. At last AlN seems to be the most promising candidate material for thermal management.

The thermal conductivity of AlN ceramics is greatly influenced by its chemical purity and density, while the theoretical value is predicted to be 320 W/mK at room temperature. Especially, a small amount of oxygen impurity markedly decreases thermal conductivity as shown in Fig. 1.

2. AlN Substrate Properties

Typical properties for the AlN substrate are summarized in Table 2. Table 2 compares properties for AlN and other substrates (Al_2O_3, BeO, SiC) at room temperature.

The AlN substrate has a maximum thermal conductivity of 240~260 W/mK at room temperature, which is over 12 times as high as that of Al_2O_3 and 80% of the theoretical value.

The AlN substrate shows excellent thermal expansion matching to the silicon chip. The thermal expansion coefficient is closer to that of silicon than those of Al_2O_3 and BeO. As a result, there is little stress problem induced by thermal mismatch between silicon chip and AlN substrate.

The AlN substrate also has good electrical properties, as good as Al_2O_3 and BeO. It shows high electrical insulation resistivity, and low dielectric constant and loss, though SiC has the disadvantages of extremely high dielectric constant and loss [1].

The AlN substrate shows not only higher flexural strength but also easier machinable property than Al_2O_3. The flexural strength at room temperature is 3500~4000 kg/cm^2, which is higher than those of Al_2O_3 and BeO. On the other hand, the vickers hardness is 1200 kg/mm^2.

3. Development of Multilayer AlN Substrates

A co-fired multilayer AlN substrate is the significant breakthrough for AlN substrate application. Multilayer AlN substrates were successfully developed by co-firing the AlN green sheets with W conductor pastes.

The multilayer structure was achieved by laminating tape-cast AlN green sheets screen-printed with W thick-film paste. The W paste included 3 wt% AlN powder to make the fired shrinkage of W close to that of the AlN. The laminated body was fired at 1900°C under 0.1 MPa N_2 gas for 4h. Densification of AlN was achieved by 2 wt% CaC_2 sintering aids.

Figure 2 shows the test samples of multilayer AlN substrates, which were used to evaluate electrical resistivities of external and internal conductors, adhesion property of the external conductor and camber of the substrate. Characteristics for the test sample are summarized in Table 3. Sheet resistivities of external and internal conductors are 20 and 25 mΩ/□, respectively. These values are satisfactory for practical use. The adhesion strength, measured by nailhead pull test of pins soldered onto 2-mm Ni-plated square pads, was more than 20 MPa, which is adequate for practical uses. In addition, the camber of the multilayer AlN substrate was measured to investigate any shrinkage mismatch between the AlN substrate and the W conductor. The camber of 20 μm/20 mm is as well as that of the standard AlN substrate. These preliminary results indicate that the multilayer AlN substrate is feasible for use in place of a conventional Al_2O_3 package.

In Fig. 2, 5 external conductor lines on the AlN green body can be seen. After firing, 7 internal conductor lines on the 2nd AlN layer appear in sight, because the AlN substrate is translucent. Another multilayer AlN substrate, with 3 metallized layers, is shown in Fig. 3. Circuit density for the multilayer AlN substrate is extremely higher than that of the test sample. It is an example of a multichip package (MCP), which is capable of mounting 10 LSI chips.

4. Characterization of Multilayer AlN Substrates [11]

(1) Optical Microscopy

The cross-sectional image in Fig. 4 shows a typical AlN and W layer structure. The thickness of AlN ad W were 120 and 5 to 10 μm, respectively, and the AlN ceramics were very dense. On the other hand, the W layers included many small dark spots. Interface morphology was irregular, but there was excellent contact between the W and AlN.

(2) Cross-Sectional SEM Observation and EDX Analysis

The polished section (Fig. 5(a)) shows nearly pore-free AlN and W phases. As will be shown later, the second phase (A) within the conductor layer has a high Al content and is probably the AlN intentionally added to the W paste. Although the interface is very rough and irregular, excellent conformity developed between the AlN and W during sintering, and a complex interlocking interface structure was found (B). The interface was sharp and clean without any apparent reaction phases.

An electron microprobe analysis on the SEM was used to obtain chemical analysis of the compositional variation of Al and W. Figure 6(a) shows a cross-sectional SEM image and Fig. 6(b) electron microprobe elemental profiles along the line shown in Fig. 6(a). The microprobe data of Fig. 6(b) shows that there was no interdiffusion of either Al or W at the interface or at the isolated Al compound particle in the W layer at the order of a few micrometers. The size of this particle (about 1 μm) is very close to that of the starting raw AlN powder added to the W paste. Therefore these particles are presumed to be AlN phase. In addition, several intricate interfaces (A) and a particle connected by a neck (B) to the AlN ceramic layer were also observed.

(3) Interface Morphology

Several intricate or interlocked interfaces were found in cross-sectional optical microscope and SEM images. To investigate in more detail the interface morphology, the W pad was removed from the substrate using NaOH etchant, and the planar interface was observed directly in the SEM. W surface morphologies at the surface side and at the W-AlN interface side are shown in Figs. 7(a) and (b), respectively.

It became apparent that W surface morphology at the interface side was very rough and had a smaller grain microstructure compared with that at the surface side. These facts indicate W grain growth at the interface was depressed by cofiring AlN and W, and the interlocking structure of AlN exists at the entire interface.

(4) Cross-Sectional TEM Observations (XTEM)

An XTEM procedure was used to analyze the structure and chemistry at the interface. The W conductor lines remained as long W bridges in the ion-milled specimens because of differences in the ion-milling rate between AlN and W. Figure 8 shows an XTEM micrograph (at 100 kV) at the AlN-W-AlN interface where most of the AlN was milled away and the much thicker W remains.

Figure 8 illustrates several distinctive features. First, there are several holes in the W layer. They may be either intrinsic holes or extrinsic holes which are related to ion-milling perforation of AlN particles. The interface morphology in the TEM image also shows characteristic intricate interlocking structures (A). Second, although most of the interface is a very tight structure, there is a small pore (B) and an opening (C) at the interface. These are the only pores observed. However, if such pores or openings are intrinsic and exist extensively at the interface, the interface might then have a poor vacuum-tight seal property.

Bright- and dark-field TEM images at higher magnification and SAD patterns taken from two grains, A and B, adjacent to each other are shown in Fig. 9. The bright-field image includes an electron transparent region (A) and a dark region (B). There were some small particles which were identified using scanning transmission electron microscopy and energy-dispersive X-ray analysis (STEM/EDAX) to be W contamination particles deposited during ion milling. The selected-area electron diffraction (SAD) patterns and corresponding dark-field images from regions A and B are shown in Figs. 9(b) and (c), respectively. The SAD patterns from regions A and B were indexed to be $Z=[1\bar{2}1\bar{3}]$ of AlN and $Z=[\bar{1}33]$ of W, respectively. These dark-field images reveal that there is no secondary phase between the AlN and W phases. Consequently, it was concluded that there was no reaction between AlN and W to yield any new phase to account for high adhesion strength at the interface.

Figure 10 is an STEM image of the W-AlN interface taken at 200 kV. Again, no interface phase was visible between the W and AlN. An EDAX scan with a spot size of 40 nm was conducted along the line shown in Fig. 10, and the signal traces for Al and W are shown in Fig. 11. The W signal was significant up to 200 nm into the AlN, indicating some diffusion of W across the interface.

5. Summary

Multilayer AlN substrates have been developed by co-firing AlN greensheets screen-printed with W thick-film paste. The properties of the substrates, such as electrical resistivity and adhesion of W conductor and the camber of the substrate, were satisfactory for practical use. The AlN-W interfaces in the co-fired AlN substrate were characterized using optical microscopy, SEM and TEM. A cross-sectional optical image showed the AlN ceramics were very dense and the thickness of AlN and W layers were 120 and 5 to 10 μm, respectively. Cross-sectional SEM micrographs of the polished and fractured interfaces indicated that the intentionally added AlN particles remained intact in particles in the W layer, and a fully sintered, interlocked AlN-W grain structure developed at the AlN-W interface. Electron microprobe analyses using SEM showed that there was no diffusion of either Al or W at the interface at the order of a few micrometers. However, using an STEM with a spot size of 40 nm, a slight diffusion layer of W could be detected up to 200 nm into the AlN. It was found that W surface morphologies at the interface side were very rough, with a small grain microstructure compared with the surface side. The interlocked AlN grains at the interface existed at the entire interface. Cross-sectional TEM observation also showed intricate microstructure at the interface, and bright-field and dark-field images and SAD patterns revealed that there was no secondary phase between AlN and W phases.

Consequently, it was concluded that the high adhesion strength of W layers onto the AlN substrate (>20 MPa) was not attributed to any secondary phase but to mechanical interlocking of AlN powder during cofiring AlN and W powders.

Acknowledgements

Characterization of the AlN-W interface was carried out in collaboration with Dr. William D. Scott and Cetin Toy at the University of Washington, USA.

References

[1] S. Ogihara, T. Yasuda, K. Otsuka and F. Kobayashi, "Application to LSI Packages of SiC Ceramics with High Thermal Conductivity," Proc. 3rd Internat. Microelectronics Conf., 1984, p. 423-427.

[2] N. Iwase, A. Tsuge and Y. Sugiura, "Development of a High Thermal Conductive AlN Ceramic Substrate Technology," ibid., 1984, p .180-185.

[3] W. Werdecker and F. Aldinger, "High Performance Aluminum Nitride Substrate by Tape Casting Technology," Proc. 35th Electronic Components Conf., 1984, p. 26-31.

[4] N. Kuramoto and H. Taniguchi, "Transparent AlN Ceramics," J. Mater. Sci. Lett., 3, 1984, p. 471-474.

[5] Y. Kurokawa, K. Utsumi, H. Takamizawa, T. Kamata and S. Noguchi, "AlN Substrates with High Thermal Conductivity," IEEE Trans. Components, Hybrids and Manufacturing Technology, CHMT-8, 2, June 1985, p. 247-252.

[6] Y. Kurokawa, H. Hamaguchi, Y. Shimada, K. Utsumi, H. Takamizawa, T. Kamata and S. Noguchi, "Development of Highly Thermal Conductive AlN Substrate by Green Sheet Technology," Proc. 36th Electronic Components Conf., 1986, p. 412-418.

[7] N. Kuramoto, H. Taniguchi and I. Aso, "Translucent AlN Ceramic Substrate," ibid., 1986, p. 424-429.

[8] N. Iwase, T. Yanazawa, M. Nakahashi, K. Shinozaki, A. Tsuge and K. Anzai, "Aluminum Nitride Multilayer Pin Grid Array Packages," Proc. 37th Electronic Components Conf., 1987, p. 384-391.

[9] N. Iwase, K. Anzai and K. Shinozaki, "Aluminum Nitride Substrates Having High Thermal Conductivity," Solid State Technology, vol.29, No. 10, 1986, p.135-138.

[10] Y. Kurokawa, H. Hamaguchi, Y. Shimada, K. Utsumi and H. Takamizawa, "Highly Thermal Conductive Aluminum Nitrides," Proc. ISHM 1987, p. 654-661.

[11] Y. Kurokawa, C. Toy and William D. Scott, "Characterization of the AlN-W Interface in a Confired Multilayer AlN Substrate," J. Am. Ceram. Soc., 72 [4] p. 612-616, 1989.

Table 1 Recent trend in the development of high thermal conductivity substrates

Year	Company	Material	Thermal Conductivity	Topics
1982	Hitachi	SiC	270w/mK	——
1983	Toshiba	AlN	60	Thyristor for Train
1984	Hitachi	SiC	270	ECL LSI Package
	Toshiba	AlN	100	Y_2O_3 Additive
	Tokuyama Soda	AlN	110	High Purity AlN Powder Translucent AlN
	Heraeus	AlN	140~170	——
	NEC	AlN	160	Reducing Sintering
	NEC	AlN	160	Transistor, LED, Laser Diode
1985	Sumitomo Denko	AlN	220	——
1986	NEC	AlN	240~260	CaC_2 Reductant
	NEC	AlN	160	Multilayer Substrate
	Tokuyama Soda	AlN	260	——
1987	Toshiba	AlN	260	Reducing Atmosphere
	Toshiba	AlN	70	Multilayer PGA

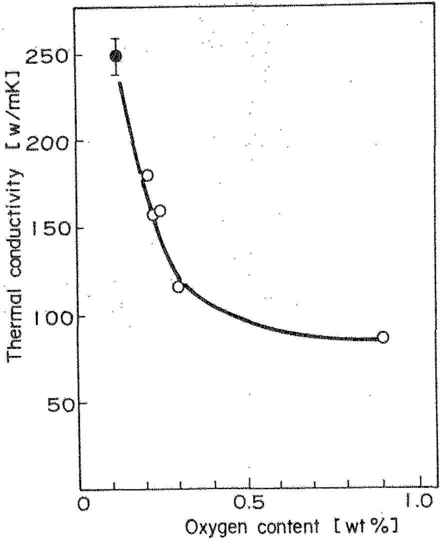

Fig. 1 Relation between thermal conductivity and oxygen content of AlN ceramics.

Table 2 Properties for AlN and other substrates at room temperature

Properties \ Substrates	NEC-AlN	96%Al_2O_3	99.5%BeO	SiC
Thermal Conductivity (W/mK)	160~260	20	260	270
Thermal Expansion Coefficient (r.t.~400 °C) ($\times10^{-6}$/°C)	4.3	6.7	7.5	3.7
Electrical Resistivity (Ωcm)	$>10^{13}$	$>10^{13}$	$>10^{13}$	$>10^{13}$
Dielectric Constant at 1MHz	8.9	8.9	6.7	42
Dielectric Loss($\times10^{-4}$) at 1MHz	1	2	1	500
Flexural Strength (Kg/cm^2)	3500~4000	3000	2500	4500
Vickers Hardness (Kg/mm^2)	1200	3000	1200	3000

Thermal expansion coefficient of Si is 3.5~4.0 $\times10^{-6}$/°C.

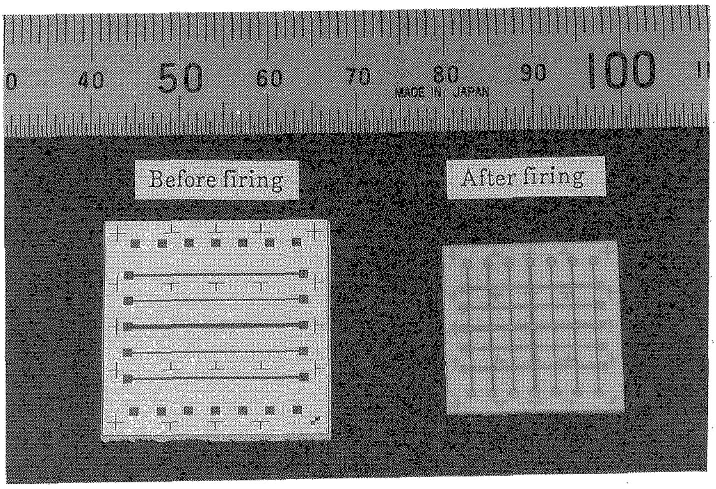

Fig. 2 Test samples for the multilayer AlN substrates.

Table 3 Characteristics for the multilayer AlN substrate with co-fired W conductors

Test		Result
Sheet resistivity	External conductor	20mΩ/□
	Internal conductor	25mΩ/□
Adhesion strength		$>$ 2 kg/mm^2
Camber		20 μm/20 mm

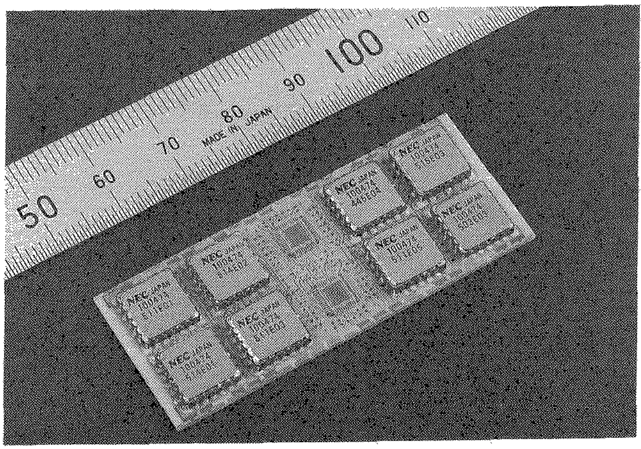

Fig. 3 Multilayer AlN substrate with 3 metallized layers.

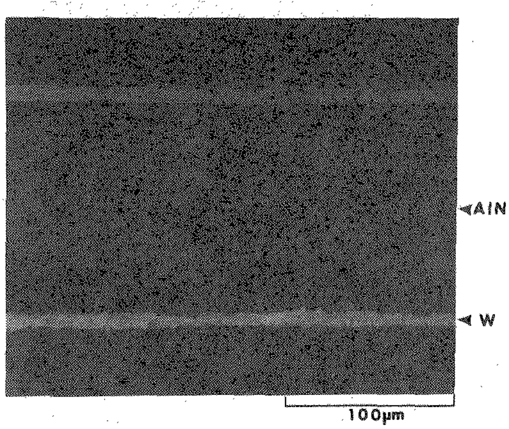

Fig.4 An optical microscope image of the cross section of the co-fired multilayer AlN substrate.

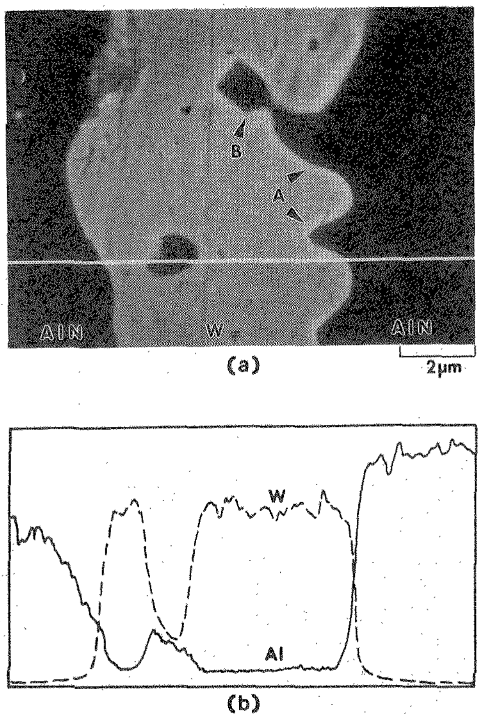

Fig.6 Cross-sectional SEM image (a) and electron microprobe elemental profiles (b) at the AlN/W/AlN interface.

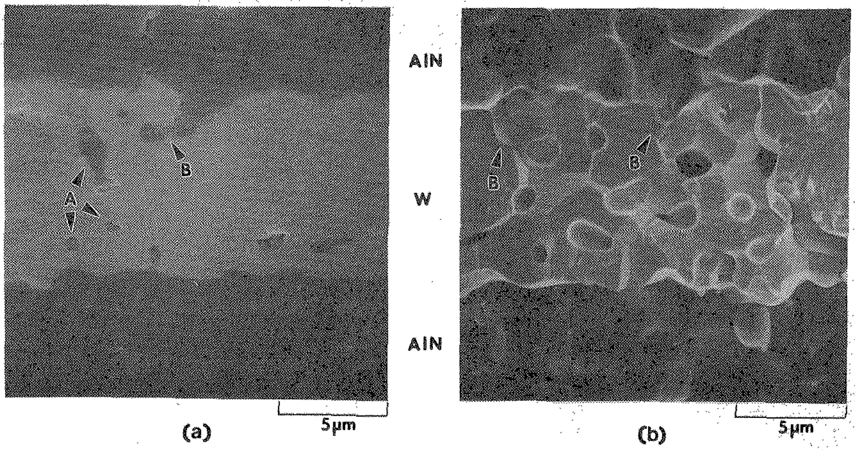

Fig.5 SEM micrographs of cross sections of AlN/W/AlN interface.
(a) Polished section
(b) Fractured section

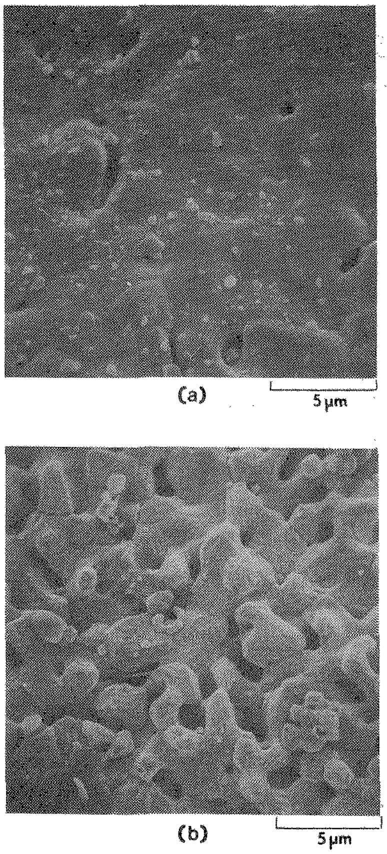

Fig. 7 Surface morphologies of the W pad.
(a) External surface side
(b) W/AlN interface side

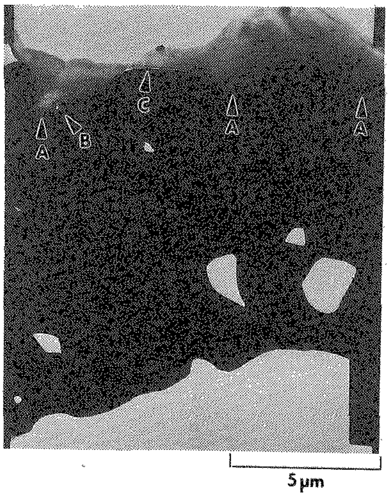

Fig. 8 Cross-sectional TEM micrograph at the AlN/W/AlN interface.

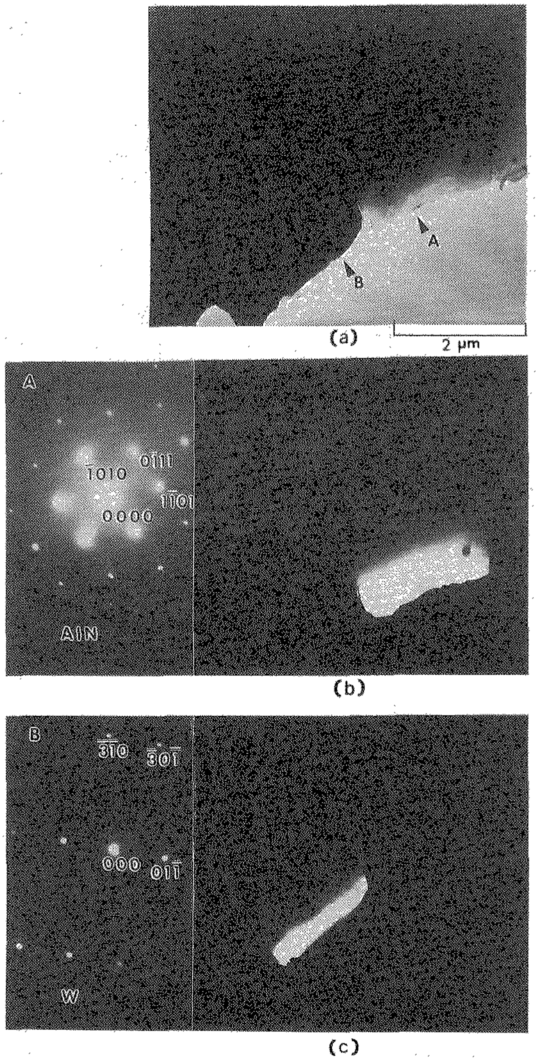

Fig. 9 TEM images and SAD patterns at the AlN-W interface
(a) BF image
(b) SAD pattern and DF image from region B.
(c) SAD pattern and DF image from region C.

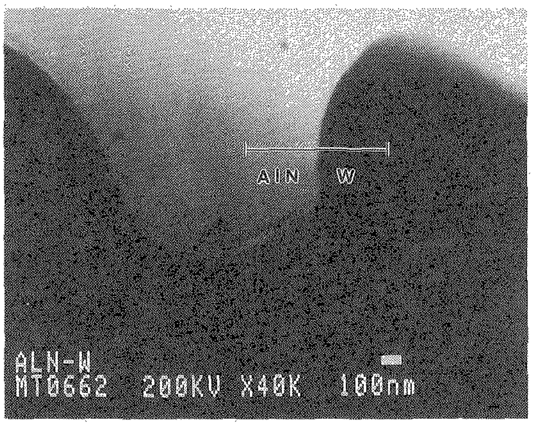

Fig. 10 STEM image showing the location of the linescan in Fig. 11

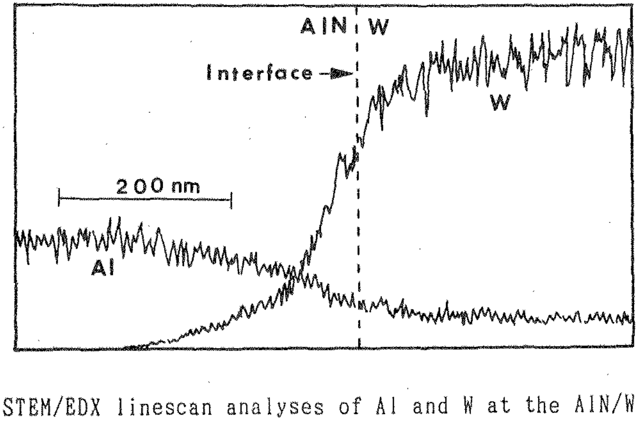

Fig. 11 STEM/EDX linescan analyses of Al and W at the AlN/W interface.